Beam dynamics in quadratically nonlinear waveguides with gain and losses

E. N. Tsoy, F. Kh. Abdullaev, and V. E. Eshniyazov

Physical-Technical Institute of the Uzbek Academy of Sciences, Bodomzor Yuli St. 2-B, Tashkent-84, Uzbekistan

A propagation of optical beams in active waveguides with quadratic nonlinearity is considered. It is shown that gain in one harmonic can compensate losses in the other harmonic. As a result of this process, stationary beams can be formed in the system. Exact solutions for stationary modes of a single waveguide are obtained, and their stability is analyzed. A possibility of the Hopf bifurcation that results in emergence of stable periodic regimes in a monomer is demonstrated. Stationary solutions are also found for a dimer with identical waveguides and a dimer with parity-time symmetry. The stability analysis demonstrates that stable beams exist in a wide range of the system parameters.

I. INTRODUCTION

Media without inversion symmetry are characterized by quadratic optical nonlinearity. When light at frequency ω propagates in such media, it generates a wave at double frequency. This process of second harmonic generation (SHG) has been realized experimentally by using cw beams and pulses, in bulk media and waveguides [1–3]. This effect is used in many applications, such as frequency conversion and amplification.

Recently it was suggested to use distributed (in transverse directions) gain and losses to provide an additional control of properties of optical systems, see reviews [4,5]. Systems with parity-time ($\mathcal{PT}$) symmetry belong to this type, and now they are actively studied [4,5]. The idea came from analysis of non-Hermitian Hamiltonian systems in quantum mechanics [6,7]. The main property of $\mathcal{PT}$-symmetric systems is their invariance with respect to consecutive transformations $\mathbf{r} \to -\mathbf{r}$ and $t \to -t$ (together with complex conjugation). Gain and losses in $\mathcal{PT}$-symmetric systems are distributed in a balanced way, such that these systems may support stable stationary modes.

A basic $\mathcal{PT}$-symmetric model that involves quadratic ($\chi^{(2)}$) nonlinearity is studied in Ref. [8]. This model consists of two $\chi^{(2)}$ waveguides with linear coupling. One waveguide has gain for both harmonics, while the other waveguide has losses. Stationary nonlinear modes, their stability, and solitons are analyzed in Refs. [8–10]. Also, related questions of wave mixing in $\mathcal{PT}$-symmetric quadratic media are considered in Refs. [11–13].

A motivation of the present paper is to consider a model alternative to that studied in Ref. [8]. Namely, we study two waveguides, where each waveguide has gain in one harmonic and losses in the other harmonic. We refer to these waveguides as active waveguides. Even a single active waveguide demonstrates interesting properties. Therefore, first we analyze stationary states and their stability in a single waveguide. The amplitude and the propagation constant of stationary states are fixed by the system parameters, which is typical for dissipative systems. We identify the presence of the Hopf

bifurcation, when a stationary state becomes unstable, and a periodic state emerges. Then we study a $\chi^{(2)}$ dimer in a $\mathcal{PT}$-symmetric case and in a general setup. For a $\mathcal{PT}$-symmetric dimer, we find a family of stationary modes, parameterized by the total intensity. Also, exact solutions for stationary modes in a symmetric $\chi^{(2)}$ dimer are found. Numerical simulations of dimers demonstrate also an existence of periodic and chaotic regimes.

II. A SINGLE ACTIVE WAVEGUIDE

Let us consider a $\chi^{(2)}$ waveguide with resonance atoms pumped, for example, from a side at ω or 2ω. A pump provides gain at corresponding frequency. This model in the cw regime is described by the following equations [1,14,15]:

$$
\begin{aligned}
i u_z - \alpha u + u^* v + i\gamma u &= 0, \\
i v_z - \beta v + \tfrac{1}{2} u^2 - i\delta v &= 0,
\end{aligned}
\tag{1}
$$

where u and v are the envelopes of the fundamental wave (FW) and the second harmonic (SH), respectively, and z is the longitudinal coordinate that plays the role of the evolutional variable. A star means complex conjugation. Positive (negative) γ and δ correspond to losses (gain) in the FW and gain (losses) in SH.

Equations (1) are written in dimensionless form. A characteristic length scale l_s on z is defined as [1]

$$
l_s = \frac{n_1 c^{3/2}}{\omega_1 d_{\text{eff}}} \left(\frac{\epsilon_0 n_2}{4 I_{1s}} \right)^{1/2},
\tag{2}
$$

where ω_1 is the frequency of FW, d_{eff} is the effective parameter of the second-order nonlinearity [1], $n_{1,2} \equiv n(\omega_{1,2})$, $n(\omega)$ is the refractive index, and I_{1s} is the intensity scale of FW. Parameter $\alpha = l_s(k_1 - k_0)$ is a shift of wave number k_1 from some reference wave number k_0, while β is related to the phase mismatch $\Delta k = 2k_1 - k_2$ as $\beta = l_s \Delta k + 2\alpha$. By setting $k_0 = k_1$, one can eliminate parameter α; however, we prefer to treat Eqs. (1) in a more general form. Variables u and v are scaled such that $|u|^2$ and $|v|^2$ are dimensionless intensities. The intensity scale of SH is defined as $I_{2s} = 2I_{1s}$.

Model (1) was considered previously, for example, in Refs. [14] and [15] within the context of an amplifier. Namely, the authors of Refs. [14] and [15] suggested to amplify the FW by introducing gain in the SH. However, only a case with gain in SH (positive γ and δ) has been considered, and analytical solutions have not been presented in these works.

By changing the intensity of the external pump, one can modify the gain parameter (δ when $\delta > 0$, or γ when $\gamma < 0$). Therefore, light propagation in model (1) can be controlled optically. The aim of this section is to analyze the main properties of model (1) for different system parameters. In particular, we demonstrate that this model behaves as a forced dissipative oscillator and it has stationary, periodic, and infinitely growing states.

A. Stationary solutions

In general, total intensity $P = |u|^2 + 2|v|^2$ is not conserved:

$$P_z = -2(\gamma|u|^2 - 2\delta|v|^2). \tag{3}$$

However, when the right-hand side turns to zero, P is constant. This can be realized when $|u(z)|$ and $|v(z)|$ are constant. Also, when $|u(z)|$ and $|v(z)|$ are periodic, P can remain finite. We show that both these cases are realized in the system.

We look for a solution in the form

$$u = Ae^{i\mu z}, \quad v = Be^{2i\mu z}, \tag{4}$$

where amplitude A and propagation constant μ are real parameters, while B is complex. Then, we get the following solution:

$$A = \pm\sqrt{2\gamma\delta(F^2 + 1)}, \quad B = \gamma(F - i), \tag{5}$$

where

$$\mu = \frac{\beta\gamma - \alpha\delta}{\delta - 2\gamma}, \quad F = \frac{\beta - 2\alpha}{\delta - 2\gamma}.$$

This solution is valid, when $\gamma\delta > 0$ and $\delta \neq 2\gamma$. In fact, solution (4) represents a family of solutions, because if $[u(z), v(z)]$ is a solution, then $[u(z)\exp(i\phi), v(z)\exp(2i\phi)]$ is also a solution, where ϕ is an arbitrary constant phase. A presence of stationary solutions with parameters that depend only on the system parameters suggests an important application of an active monomer as an amplitude filter or a limiter.

B. Stability of stationary solutions

Now we check the stability of stationary modes. For this purpose, we substitute

$$u = [A + a(z)]e^{i\mu z}, \quad v = [B + b(z)]e^{2i\mu z} \tag{6}$$

into Eqs. (1) and obtain equations for small modulations $a(z)$ and $b(z)$. Separating the real and imaginary parts of $a(z)$ and $b(z)$, and representing them as $\sim \exp(\eta z)$, we get a linear set of four algebraic equations for modulation components. This set has a nontrivial solution when determinant D is zero:

$$D(\eta) \equiv \eta(\eta^3 + s_1\eta^2 + s_2\eta + s_3) = 0, \tag{7}$$
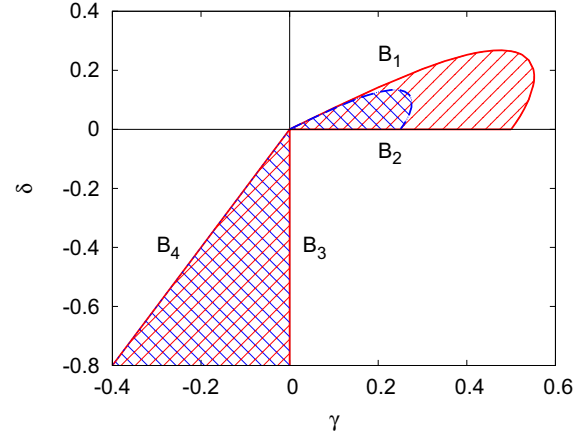

FIG. 1. Shaded regions correspond to regions of stability of stationary mode (4). A solid (dashed) line corresponds to $\alpha = 0$ and $\beta = 1$ ($\beta = 0.5$). Labels B_j, $j = 1, \ldots, 4$, indicate boundaries of the stability regions.

where

$$s_1 = 2(\gamma - \delta),$$
$$s_2 = \delta[\delta + (4\gamma + \delta)F^2],$$
$$s_3 = 2\gamma\delta(2\gamma - \delta)(F^2 + 1). \tag{8}$$

Stationary solution (4) is stable when all roots of $D(\eta)$ are in the left half of the complex η plane. One root of $D(\eta)$ is always zero. The roots of $\widetilde{D}(\eta)$, where $D(\eta) = \eta\widetilde{D}(\eta)$, have negative real parts, when

$$s_1 > 0, \quad s_3 > 0, \quad \text{and} \quad s_1 s_2 > s_3. \tag{9}$$

Figure 1 shows the regions of stability of stationary modes (4) in the (γ, δ) plane for $\alpha = 0$ and two values of β. The shaded regions in Fig. 1 correspond to the parameters of stable modes. Double-shaded regions mean overlapping of regions for $\beta = 0.5$ and $\beta = 1$. When β decreases, the region in the first quadrant shrinks to zero while that in the third quadrant does not depend on β (for $\alpha = 0$).

Boundary B_1 corresponds to the third condition in Eqs. (9). At boundary B_1 function $\widetilde{D}(\eta)$ has two pure imaginary (conjugate) roots, and therefore the supercritical Hopf bifurcation occurs at these values of the parameters. Stationary mode (4) becomes unstable, and a stable limit cycle emerges. This means that near B_1, outside the stability domain, the variation of $u(z)$ and $v(z)$ is periodic.

However, this periodic dynamics becomes quickly unstable for larger values of δ. This is due to merging of the stable and unstable limit cycles. The physical meaning of this transition is that energy cannot be utilized effectively in the FW due to very high gain in the SH. In contrast, for small δ, the stable limit cycle exists at γ well beyond B_1.

Figure 2 shows the dependence of field intensities on z. The following initial conditions $u(0) = 1$ and $v(0) = 0$ are used. For parameters inside the stability region, $\gamma = 0.3$ and $\delta = 0.1$, the dynamics tends to the stationary mode [see Fig. 2(a)]. When $\gamma = 0.6$ and $\delta = 0.1$, the stationary state is unstable and the dynamics is periodic [see Fig. 2(b)]. Figure 2(c) demonstrates a case when periodic oscillations
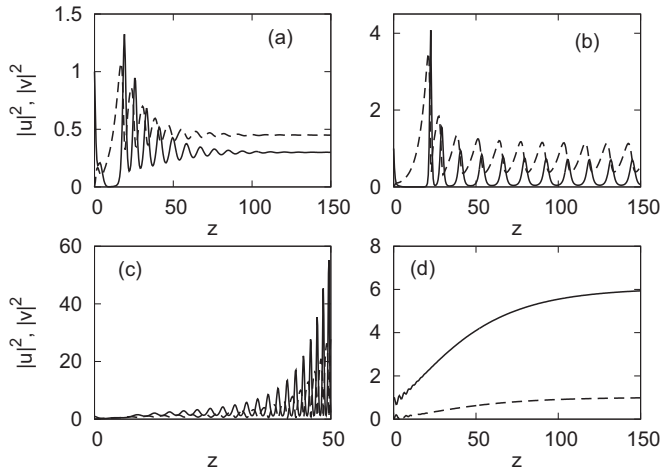
FIG. 2. Variation of FW (solid lines) and SH (dashed lines) on z. (a) Transition to a stationary state at $\gamma = 0.3$ and $\delta = 0.1$, (b) transition to a periodic state at $\gamma = 0.6$ and $\delta = 0.1$, (c) an infinite growth at $\gamma = 0.3$ and $\delta = 0.3$, and (d) transition to a stationary state at $\gamma = -0.1$ and $\delta = -0.3$. Other parameters are $\alpha = 0$ and $\beta = 1$.

become unstable. Parameter γ in Fig. 2(c) is the same as in Fig. 2(a), but a larger value of gain δ results in an infinite growth of both modes.

At boundary B_2 (a segment on $\delta = 0$ line), two roots of $\widetilde{D}(\eta)$ are simultaneously zero. When $\gamma > 0$ and $\delta < 0$ [in the fourth quadrant of the (γ, δ) plane], solution (4) is not valid. For these parameters, both FW and SH experience losses. Therefore, asymptotically both $|u|$ and $|v|$ vanish to zero.

At boundary B_3, only a single real root turns to zero. At B_4, $\delta = 2\gamma$, all $|u|$, $|v|$, and μ diverge. Nevertheless, inside the stability region, gain in the FW can compensate losses in the SH, and high amplitudes of the SH can be realized. A typical example of the dynamics in this region is shown in Fig. 2(d). After a transition process, both modes tend to stationary states. By changing parameters to boundary B_4, the amplitudes of modes increase, diverging on B_4. Also, it is necessary to remember that just near B_4, one eigenvalue η is small so that longer structures are necessary to achieve the stationary regime. On the left side from B_4, both modes grow exponentially.

We also mention that additional care should be taken in analysis of the cascading limit of Eqs. (1). In the conservative model, $\gamma = \delta = 0$, when the mismatch parameter β is large, the first term in the equation for SH is ignored [16]. This gives $v = u^2/(2\beta)$. Substituting the last equation to the first of Eqs. (1), we obtain for u the equation with cubic nonlinearity. If we apply a similar procedure to Eqs. (1) with $\gamma, \delta \neq 0$, we get

$$(|u|^2)_z + 2\gamma |u|^2 - \frac{\delta}{\beta^2 + \delta^2} |u|^4 = 0. \tag{10}$$

This equation predicts unstable (stable) stationary solutions for the whole region where γ and δ are positive (negative). This result contradicts the stability analysis, presented above. The reason is that one cannot simply drop v_z, because $v_z \sim \mu$ can be large for large β.
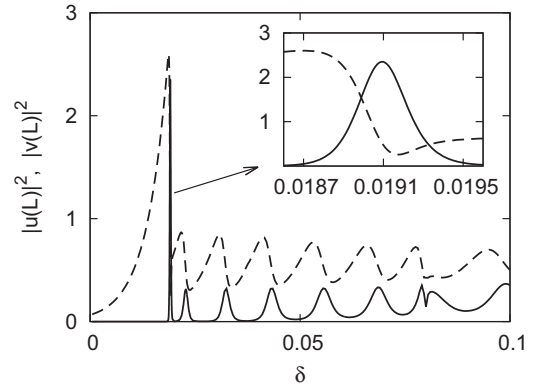

FIG. 3. The dependence of output on the gain parameter for $L = 100$, $\gamma = 0.5$, $\alpha = 0$, and $\beta = 1$. The inset represents a magnified view of the first peak.

C. Finite waveguides

Now we analyze a possibility to control the system properties by changing the gain parameter. The latter can be done by varying the intensity of the external pump. We consider a structure of finite length L, and we find the output fields, solving Eqs. (1) numerically. The input is the same as in Fig. 2. Figure 3 shows the dependence of the output as a function of the gain parameter for $L = 100$ and $\gamma = 0.5$. This dependence is represented by a sequence of peaks. The inset in Fig. 3 shows the first peak. One can see that by varying the gain parameter by $\sim 2\%$–3%, one can strongly modify the output.

The analysis for different values of L, γ, and δ results in the following findings. Typically, the first (on δ) peak, as more narrow and higher, can be used for applications. An increase of L at fixed γ results usually in a decrease of both the peak position on δ and its amplitude. In contrast, when γ increases at fixed L, the peak position shifts to the right and its amplitude increases.

Let us estimate real values of the parameters. A typical length of a crystal or a waveguide for SHG is 5 cm [2,3,17,18]. It follows from Fig. 2 that the transition to a stationary state occurs at $z \sim 10$–50, and therefore scale $l_s \sim 1$–5 mm. For media with a nonlinear parameter $d_{eff} \sim 10^{-11}$ pm/V, such l_s can be achieved for $I_s \sim 10$–100 MW/cm^2 [see Eq. (2)]. Such intensities are available from pulsed lasers [17,18]. For sufficiently long (micro- or nanoseconds) pulses and the high repetition rate, the time-independent dynamics can be realized. Materials such as KTP and LiNbO$_3$ have the required value of nonlinearity for a proper direction [1], while the optical damage threshold is > 1–100 GW/cm^2 (see, e.g., Ref. [17]). By changing the direction of the beam propagation, one can tune the phase-matching parameter Δk, and therefore β. Values of losses of untreated crystals for SHG are of order 1–10 m^{-1}, which gives $|\gamma|$, $|\delta| \sim 10^{-2}$–10^{-3} (see, e.g., Ref. [18]). However, these parameters can be modified by introducing resonance atoms, which provide additional absorption, to a crystal. Therefore, effects discussed in this work can be realized experimentally by using modern laser sources and materials.

III. A DIMER OF ACTIVE WAVEGUIDES

Now we consider two coupled $\chi^{(2)}$ waveguides (a $\chi^{(2)}$ dimer). This system is described by the following set of equations:

$$
iu_{n,z} - \alpha_n u_n + u_n^* v_n + i\gamma_n u_n = \kappa_u u_{3-n},
$$

$$
iv_{n,z} - \beta_n v_n + \frac{1}{2}u_n^2 - i\delta_n v_n = \kappa_v v_{3-n}, \qquad (11)
$$

where κ_u (κ_v) is the coupling parameter for the FW (SH), and $n = 1$ and 2. This system in the absence of gain and losses ($\gamma_n = \delta_n = 0$) was studied, for example, in Ref. [19]. A special type of $\mathcal{PT}$-symmetric coupler with three-wave interaction is presented in Ref. [11].

When $\gamma_1 = -\gamma_2$, $\delta_1 = -\delta_2$, and $\gamma_1\delta_1 < 0$ (values in the second and fourth quadrants of Fig. 1), the system is $\mathcal{PT}$ symmetric, and it was studied in Ref. [8]. Here we study an alternative $\mathcal{PT}$-symmetric dimer, when $\gamma_1 = -\gamma_2$, $\delta_1 = -\delta_2$, and $\gamma_1\delta_1 > 0$ (values in the first and third quadrants). Also, symmetric dimers and asymmetric dimers are analyzed.

A. A $\mathcal{PT}$-symmetric dimer,
$\alpha_1 = \alpha_2 = \alpha$, $\beta_1 = \beta_2 = \beta$, $\gamma_1 = -\gamma_2 = \gamma$, and $\delta_1 = -\delta_2 = \delta$

First, let us consider a linear $\mathcal{PT}$-symmetric system (11). Looking for a solution in the form $u_n = A_n \exp(i\mu z)$ and $v_n = B_n \exp(2i\mu z)$, we arrive to a linear eigenvalue problem for parameter μ. Then the linear eigenvalues have the following form [8]:

$$
\mu_{1,2} = -\alpha \pm \sqrt{\kappa_u^2 - \gamma^2},
$$

$$
\mu_{3,4} = \frac{1}{2}\left(-\beta \pm \sqrt{\kappa_v^2 - \delta^2}\right). \qquad (12)
$$

When $|\gamma| > |\kappa_u|$ or $|\delta| > |\kappa_v|$, a linear dimer has broken $\mathcal{PT}$ symmetry [8]. Besides the $\mathcal{PT}$-symmetry thresholds, Eqs. (12) provide values of the propagation constant, from which nonlinear stationary states bifurcate.

We look for stationary solutions in the following form:

$$
u_1 = Ae^{i\mu z}, \quad v_1 = Be^{2i\mu z},
$$

$$
u_2 = A^* e^{i\mu z}, \quad v_2 = B^* e^{2i\mu z}, \qquad (13)
$$

where amplitudes of modes in different waveguides are taken in $\mathcal{PT}$-invariant form. Representing complex amplitude A as $A = |A|\exp(i\phi)$, one can express B and $|A|$ as functions of ϕ:

$$
B = (\mu + \alpha - i\gamma)e^{2i\phi} + \kappa_u, \qquad (14)
$$

and

$$
|A|^2 = 2\{(\alpha + \mu)(\beta + 2\mu) + \gamma\delta
$$
$$
+ \kappa_u[(\beta + 2\mu + \kappa_v)\cos(2\phi) + \delta\sin(2\phi)]
$$
$$
+ \kappa_v[(\alpha + \mu)\cos(4\phi) + \gamma\sin(4\phi)]\}. \qquad (15)
$$

Phase ϕ is found from a single equation:

$$
(\beta + 2\mu)\gamma - (\alpha + \mu)\delta
$$
$$
- \kappa_u[\delta\cos(2\phi) - (\beta + 2\mu + \kappa_v)\sin(2\phi)]
$$
$$
- \kappa_v[\gamma\cos(4\phi) - (\mu + \alpha)\sin(4\phi)] = 0. \qquad (16)
$$

Depending on the system parameters, Eq. (16) can have from zero to four roots within one period of $\phi = [0, \pi)$. However, one should take only roots that give a positive value of $|A|^2$ in Eq. (15). When the absolute value of the free term in Eq. (16) is large enough, there are no stationary states in the system. A number of roots of Eq. (16) for a given set of parameters can easily be checked numerically.

In contrast to an active monomer, stationary solution (13) of the $\mathcal{PT}$-symmetric dimer represents a family of solutions parameterized by μ. We also mention that Eq. (16) can be considered as an equation for μ at a given value of ϕ. By doing this, one can find solutions explicitly for particular values of μ. For example, when $\phi = j\pi/4$, where $j = 0, \ldots, 3$, one can solve Eq. (16) for μ, obtaining

$$
\mu = \frac{(\kappa_v - \beta)\gamma + (\alpha \pm \kappa_u)\delta}{2\gamma - \delta} \qquad (17)
$$

for $\phi = 0$ and $\phi = \pi/2$, respectively, and

$$
\mu = \frac{-(\beta + \kappa_v)\gamma + \alpha\delta \mp (\beta + \kappa_v)\kappa_u}{2\gamma - \delta \pm 2\kappa_u} \qquad (18)
$$

for $\phi = \pi/4$ and $\phi = 3\pi/4$, respectively. Equations (17) and (18) together with Eqs. (14) and (15) give explicit stationary solutions of the dimer.

Now we can analyze the stability of stationary solutions (13). For this purpose we use

$$
u_1 = [A + a_1(z)]e^{i\mu z}, \quad v_1 = [B + b_1(z)]e^{2i\mu z},
$$

$$
u_2 = [A^* + a_2(z)]e^{i\mu z}, \quad v_2 = [B^* + b_2(z)]e^{2i\mu z}, \quad (19)
$$

where $a_n(z)$ and $b_n(z)$ are small modulations. Substituting these equations into Eqs. (11), introducing real and imaginary parts of modulations $a_n = a_{nR} + ia_{nI}$ and $b_n = b_{nR} + ib_{nI}$ and representing them as $a_{nX} = \tilde{a}_{nX}\exp(\eta z)$ and $b_{nX} = \tilde{b}_{nX}\exp(\eta z)$, where $X = R$ and I, one arrives to the following eigenvalue problem for η:

$$
\mathbf{L}(\eta)\,\psi = 0, \quad \text{where} \quad \mathbf{L}(\eta) = \begin{pmatrix} \mathbf{C}_+(\eta) & \mathbf{C}_0 \\ \mathbf{C}_0 & \mathbf{C}_-(\eta) \end{pmatrix}, \quad (20)
$$

where $\mathbf{C}_\pm$ and $\mathbf{C}_0$ are 4×4 matrices, defined as

$$
\mathbf{C}_\pm = \begin{pmatrix}
-\mu + B_R - \alpha & \pm B_I \mp \gamma - \eta & A_R & \pm A_I \\
\pm B_I \pm \gamma + \eta & -\mu - B_R - \alpha & \mp A_I & A_R \\
A_R & \mp A_I & -\beta - 2\mu & \pm\delta - \eta \\
\pm A_I & A_R & \mp\delta + \eta & -\beta - 2\mu
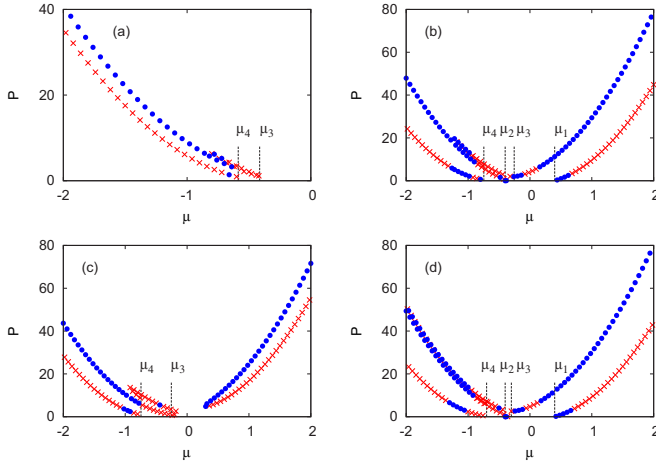\end{pmatrix} \qquad (21)
$$

FIG. 4. Stationary modes of a $\mathcal{PT}$-symmetric dimer for (a) $\gamma = 0.3$, $\delta = 0.1$, and $\kappa_u = \kappa_v = 0.2$; (b) $\gamma = 0.3$, $\delta = 0.1$, and $\kappa_u = \kappa_v = 0.5$; (c) $\gamma = 0.6$, $\delta = 0.1$, and $\kappa_u = \kappa_v = 0.5$; and (d) $\gamma = 0.3$, $\delta = 0.3$, and $\kappa_u = \kappa_v = 0.5$. Other parameters are $\alpha = 0$ and $\beta = 1$. Circles (crosses) correspond to stable (unstable) modes. Short vertical lines are positions of eigenvalues in the linear limit.

and

$$\mathbf{C}_0 = \begin{pmatrix} -\kappa_u \mathbf{I}_2 & 0 \\ 0 & -\kappa_v \mathbf{I}_2 \end{pmatrix}, \tag{22}$$

$\mathbf{I}_2$ is the 2×2 the identity matrix, and

$$\psi = (\tilde{a}_{1R}, \tilde{a}_{1I}, \tilde{b}_{1R}, \tilde{b}_{1I}, \tilde{a}_{2R}, \tilde{a}_{2I}, \tilde{b}_{2R}, \tilde{b}_{2I})^T. \tag{23}$$

In Eq. (21), notations $A = A_R + i A_I$ and $B = B_R + i B_I$ are used.

Eigenvalues are found as roots of the determinant of $\mathbf{L}(\eta)$. A stable stationary state requires the real parts of all roots to be negative. Modes of the $\mathcal{PT}$-symmetric dimer can clearly be represented in the (μ, P) plane, where $P = 2(|A|^2 + 2|B|^2)$ for stationary states (13). Stationary modes for different sets of parameters are shown in Fig. 4.

For parameters ($\gamma = 0.3$ and $\delta = 0.1$) in Fig. 4(a) and in the absence of coupling ($\kappa_u = \kappa_v = 0$), the first waveguide has a stable stationary state (see Fig. 1), while the second waveguide is in an unstable (growing) state. Parameters of coupling ($\kappa_u = \kappa_v = 0.2$) in Fig. 4(a) are taken such that $\mathcal{PT}$ symmetry is partially broken in the linear limit [see Eqs. (12)]. Nonlinear modes bifurcate from two eigenvalues of the linear system. In contrast to the linear system, there are three modes for a given P, when $P \lesssim 8$. For larger P, there are two modes, one of which is stable.

Parameters in Fig. 4(b) correspond to a case when the linear system has four eigenvalues and its $\mathcal{PT}$ symmetry is unbroken. A nonlinear dimer can have up to six modes for moderate values of $P < 20$. For high total intensity ($P > 20$), there are four modes for a given P. For low intensity ($P < 20$), modes change their stability. For high intensity ($P > 20$), modes that originate from μ_2 and μ_3 (μ_1 and μ_4) become stable (unstable).

For parameters ($\gamma = 0.6$ and $\delta = 0.1$) in Fig. 4(c), in the absence of coupling ($\kappa_u = \kappa_v = 0$), the first waveguide has a stable periodic state while the second waveguide is in an

unstable (growing) state. For $\kappa_u = \kappa_v = 0.5$, $\mathcal{PT}$ symmetry is partially broken in the linear limit. There are pure nonlinear modes in region $\mu > 0$ that emerge at finite total intensity. Similarly to the previous case, there are up to six modes for low P. For high intensity ($P > 20$), there are four modes, two of which are stable.

The parameters in Fig. 4(d) correspond to a case, when both waveguides, if decoupled, are in unstable states and the $\mathcal{PT}$ symmetry of the linear system is unbroken. The region where six modes exist is extended to higher P ($P \sim 50$). However, for high intensity $P > 50$, only four modes exist, similarly to Figs. 4(b) and 4(c). Also, for high intensity, modes that originate from μ_2 and μ_3 (μ_1 and μ_4) are stable (unstable).

Typically, an instability in Fig. 4 means an infinite growth of at least a pair of fields. We should also mention that besides stable and unstable stationary states, there are periodic and chaotic (with the finite total intensity) types of dynamics for the same values of the system parameters. These regimes are realized for different values of initial conditions.

In general, when $\gamma \delta > 0$ and the coupling is ignored, at least one waveguide in the $\mathcal{PT}$-symmetric dimer is in the unstable state. However, due to coupling, a stable stationary state can formed even in two initially unstable waveguides, as demonstrated in Fig. 4.

B. Symmetric and asymmetric dimers

Let us consider a dimer that consist of two identical waveguides, $\alpha_1 = \alpha_2 = \alpha$, $\beta_1 = \beta_2 = \beta$, $\gamma_1 = \gamma_2 = \gamma$, and $\delta_1 = \delta_2 = \delta$. We look for stationary solutions in the following form:

$$u_n = A_n e^{i\mu z}, \qquad v_n = B_n e^{2i\mu z}, \tag{24}$$

where A_n is real. Then

$$A_1 = \pm\sqrt{2\gamma\delta(F^2 + 1)}, \quad B_1 = \gamma(F - i), \tag{25}$$

where $A_2 = \sigma A_1$, $B_2 = B_1$, $\sigma = \pm 1$, and [cf. Eqs. (5) and (17)]

$$\mu = \frac{(\beta + \kappa_v)\gamma - (\alpha + \sigma\kappa_u)\delta}{\delta - 2\gamma},$$

$$F = \frac{\beta - 2\alpha - 2\sigma\kappa_u + \kappa_v}{\delta - 2\gamma}. \tag{26}$$

One can consider also a dimer with arbitrary values of γ_n and δ_n. Such a dimer is different from a $\mathcal{PT}$-symmetric dimer. In a $\mathcal{PT}$-symmetric dimer, when $\gamma_n \delta_n < 0$, both subsystems represent an unstable oscillator, while when ($\gamma_n \delta_n > 0$) at least one waveguide has an unstable stationary state. In contrast, an asymmetric dimer with $\gamma_n \delta_n > 0$ can be represented for certain parameters as a combination of two stable oscillators. Therefore, various processes of synchronization and chaotic behavior can arise in the system.

We find that in an asymmetric dimer for various values of γ_n and δ_n, provided that at least one coefficient corresponds to gain, there can be stationary or periodic states. For example, let us consider a dimer with $\alpha_1 = \alpha_2 = 0$, $\beta_1 = 1$, $\beta_2 = 0.5$, $\gamma_1 = 0.3$, $\delta_1 = 0.1$, $\gamma_2 = 0.2$, and $\delta_2 = 0.05$. In the absence of coupling, parameters of both waveguides
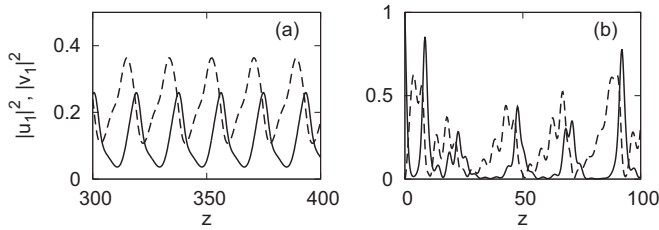
FIG. 5. Dynamics of FW (a solid line) and SH (a dashed line) in the first waveguide of the asymmetric dimer. (a) A periodic state at $\kappa_u = \kappa_v = 0.4$, and (b) a chaotic state at $\kappa_u = \kappa_v = 0.6$. Other parameters are $\alpha_1 = \alpha_2 = 0$, $\beta_1 = 1$, $\beta_2 = 0.5$, $\gamma_1 = 0.3$, $\delta_1 = 0.1$, $\gamma_2 = 0.2$, and $\delta_2 = 0.05$.

correspond to stable stationary modes, cf. Fig. 1. At weak coupling ($\kappa_u = \kappa_v = [0.01, 0.08]$), the dimer demonstrates a chaotic behavior. Then, at $\kappa_u = \kappa_v = [0.09, 0.34]$, the dimer is in a stable stationary state. At $\kappa_u = \kappa_v = [0.35, 0.52]$ and $\kappa_u = \kappa_v = [0.92, 1.3]$, the dynamics is periodic, as shown in Fig. 5(a). When $\kappa_u = \kappa_v = [0.53, 0.91]$, the dynamics again becomes chaotic, as presented in Fig. 5(b). It should be noted that a particular realization of the chaotic dynamics depends also on details of the numerical method, such as integration scheme and accuracy. For strong coupling, $\kappa_u = \kappa_v \gtrsim 1.3$, the oscillators are locked, giving a constant amplitude motion. A similar behavior is found for other values of the system parameters; however, a sequence of regimes can differ from that described above. When gain is large, the wave amplitudes grow infinitely. Therefore, dimer (11) demonstrates a rich variety of dynamics depending on the system parameters.

IV. CONCLUSION

In conclusion, we have studied the beam dynamics in a monomer and a dimer of active waveguides with quadratic

nonlinearity. It has been found that a single $\chi^{(2)}$ waveguide with gain in one harmonic and losses in the other harmonic acts as a forced dissipative oscillator. The monomer can support stationary modes, as well as periodic oscillations. The stability analysis of stationary modes of a monomer shows that for particular parameters a transition to periodic regimes is possible via the Hopf bifurcation.

It is demonstrated that the active monomer can be used as an amplitude filter, or an optically controllable switch. The variation of the gain parameter by an external pump strongly affects the transmission properties of the system. An estimate of parameters shows that these effects can be observed in waveguides of a few centimeters long, and tens of MW/cm^2 intensities, using materials with moderate second-order nonlinearity.

A set of coupled waveguides with gain and losses has also been analyzed. An alternative configuration of a $\mathcal{PT}$-symmetric dimer has been suggested. Stationary states of a dimer in $\mathcal{PT}$-symmetric and symmetric configurations have been obtained, and the stability of these states has been studied. It has been shown that stationary states of the $\mathcal{PT}$-symmetric dimer can be found from a solution of a single equation for the phase of the FW. Explicit solutions for particular values of the propagation constant μ have been obtained. For moderate values of the total intensity, the number of nonlinear modes of the dimer can be larger (up to six modes) than that in the linear system. For larger values of P, the number of modes is reduced to four, and at least two of them are stable for a wide range of the system parameters.

[1] R. W. Boyd, *Nonlinear Optics*, 3rd ed. (Academic Press, New York, 2008).

[2] C. Etrich, F. Lederer, B. A. Malomed, T. Peschel, and U. Peschel, Optical solitons in media with a quadratic nonlinearity, Prog. Opt. **41**, 483 (2000).

[3] A. V. Buryak, P. Di Trapani, D. V. Skryabin, and S. Trillo, Optical solitons due to quadratic nonlinearities: From basic physics to futuristic applications, Phys. Rep. **370**, 63 (2002).

[4] S. V. Suchkov, A. A. Sukhorukov, J. Huang, S. V. Dmitriev, C. Lee, and Y. S. Kivshar, Nonlinear switching and solitons in PT-symmetric photonic systems, Laser Photonics Rev. **10**, 177 (2016).

[5] V. V. Konotop, J. Yang, and D. A. Zezyulin, Nonlinear waves in PT-symmetric systems, Rev. Mod. Phys. **88**, 035002 (2016).

[6] C. M. Bender, Introduction to PT-symmetric quantum theory, Contemp. Phys. **46**, 277 (2005).

[7] C. M. Bender, Making sense of non-Hermitian Hamiltonians, Rep. Prog. Phys. **70**, 947 (2007).

[8] K. Li, D. A. Zezyulin, P. G. Kevrekidis, V. V. Konotop, and F. Kh. Abdullaev, PT-symmetric coupler with $\chi^{(2)}$ nonlinearity, Phys. Rev. A **88**, 053820 (2013).

[9] F. C. Moreira, F. Kh. Abdullaev, and V. V. Konotop, Localized modes in $\chi^{(2)}$ media with PT-symmetric localized potential, Phys. Rev. A **85**, 023843 (2012).

[10] M. Ögren, F. Kh. Abdullaev, and V. V. Konotop, Solitons in a PT-symmetric $\chi^{(2)}$ coupler, Opt. Lett. **42**, 4079 (2017).

[11] D. A. Antonosyan, A. S. Solntsev, and A. A. Sukhorukov, Parity-time anti-symmetric parametric amplifier, Opt. Lett. **40**, 4575 (2015).

[12] M.-A. Miri and A. Alu, Nonlinearity-induced PT-symmetry without material gain, New J. Phys. **18**, 065001 (2016).

[13] Yu. Shen, Z. Wen, Zh. Yan, and Ch. Hang, Effect of PT-symmetry on nonlinear waves for three-wave interaction models in the quadratic nonlinear media, Chaos **28**, 043104 (2018).

[14] P. L. Chu, B. A. Malomed, and G. D. Peng, Nonlinear amplification in a second-harmonic-generating system, Opt. Commun. **128**, 76 (1996).

[15] G. D. Peng, B. A. Malomed, and P. L. Chu, Soliton amplification and reshaping by a second-harmonic-generating nonlinear amplifier, J. Opt. Soc. Am. B **15**, 2462 (1998).

[16] G. I. Stegeman, D. J. Hagan, and L. Torner, $\chi^{(2)}$ cascading phenomena and their applications to all-optical signal processing,

mode-locking, pulse compression and solitons, Opt. Quantum Electron. **28**, 1691 (1996).

[17] W. E. Torruellas, Z. Wang, D. J. Hagan, E. W. Van Stryland, G. I. Stegeman, L. Torner, and C. R. Menyuk, Observation of Two-Dimensional Spatial Solitary Waves in a Quadratic Medium, Phys. Rev. Lett. **74**, 5036 (1995).

[18] R. Schick, Y. Back, and G. I. Stegeman, One-dimensional spatial solitary waves due to cascaded second-order nonlinearities in planar waveguides, Phys. Rev. E **53**, 1138 (1996).

[19] O. Bang, P. L. Christiansen, and C. B. Clausen, Stationary solutions and self-trapping in discrete quadratic nonlinear systems, Phys. Rev. E **56**, 7257 (1997).